

1 **Novel engineered chimeric engulfment receptors trigger T-cell effector functions against**  
2 **SIV infected CD4+ T cells**

3

4

5 Daniel Corey<sup>1§\*</sup>, Francoise Haeseleer<sup>2,3\*§</sup>, and Lawrence Corey<sup>1,2,3</sup>

6

7 <sup>1</sup>CERo Therapeutics, San Francisco, CA, U.S.A.

8 <sup>2</sup>Department of Laboratory Medicine, University of Washington, Seattle, WA, U.S.A.

9 <sup>3</sup>Vaccine and Infectious Disease Division, Fred Hutchinson Cancer Research Center, Seattle,  
10 WA, U.S.A.

11

12 \*Current affiliation: Outpace Bio, Seattle, WA, 98109 USA

13

14 § Authors made equal contribution

15

16 \*Correspondence should be addressed to D.C.

17 Daniel Corey

18 201 Haskins Way, Suite 230

19 South San Francisco, CA

20 94080

21 [dcorey@cerobio.com](mailto:dcorey@cerobio.com)

22

23

24 **Short title:** (50 characters; 45) CER T cells can kill SIV-infected CD4 T cells

25 **Key words:** (5-10) Chimeric engulfment receptor; SIV; HIV; CER; TIM-4; phosphatidylserine

26 **ABSTRACT**

27 Adoptive therapy with genetically engineered T cells offers potential for infectious disease  
28 treatment in immunocompromised persons. HIV/simian immunodeficiency virus (SIV) infected  
29 cells express phosphatidylserine (PS) early post-infection. We tested whether chimeric  
30 engulfment receptor (CER) T cells designed to recognize PS-expressing cells could eliminate  
31 SIV infected cells. Lentiviral CER constructs comprised of the extracellular domain of T-cell  
32 immunoglobulin and mucin domain containing 4 (TIM-4), the PS receptor, and engulfment  
33 signaling domains were transduced into primary rhesus macaque (RM) T cells. We measured  
34 PS binding and T-cell engulfment of RM CD4+ T cells infected with SIV expressing GFP. As  
35 chimeric antigen receptor (CAR) T cells induce PS and subsequent TIM-4 binding, we evaluated  
36 in vitro killing of CAR and CER T-cell combinations. We found that recombinant TIM-4 bound to  
37 SIV infected cells. In vitro, CER CD4+ T cells effectively killed SIV infected cells, which was  
38 dependent on TIM-4 binding to PS. Enhanced killing of SIV infected CD4+ T cells by CER and  
39 CAR T-cell combinations was observed. This installation of innate immune functions into T cells  
40 presents an opportunity to enhance elimination of SIV infected cells and offers potential to  
41 augment functional cure of SIV/HIV infection.

42

43

44

45

46

47

48

## 49 INTRODUCTION

50 Cell therapies are being investigated to treat a large variety of diseases. Chimeric antigen  
51 receptor (CAR) T cells are cells engineered to recognize and kill clinically relevant targets. CAR  
52 T-cell therapies are an example of successful cell therapy, especially to treat different types of  
53 hematologic malignancies<sup>1,2</sup>. New cells therapies are being investigated to broaden the number  
54 of diseases where they might be applicable and explore the potential of other effector cell types  
55 such as macrophages and natural killer cells and other CAR<sup>3-6</sup>. The application of the  
56 knowledge resulting from in vivo studies and clinical trials with CAR T cells could lead to more  
57 successful cell therapies targeting HIV reservoirs that remain in HIV-infected patients and in  
58 controlling viral rebound<sup>7-9</sup>.

59 A common feature displayed by cells that have become apoptotic because of viral or parasitic  
60 infections, aging, or altered metabolism is the redistribution of phosphatidylserine (PS) to the  
61 outer leaflet of their plasma membrane<sup>10</sup>. For example, HIV infection was shown to trigger the  
62 exposure of PS by activating scramblases<sup>11</sup>. The exposed PS was also shown to facilitate  
63 fusion between the viral and cell membrane<sup>11,12</sup>. In addition, because HIV viruses are produced  
64 by apoptotic CD4 T cells, HIV virions contain PS in their envelope that stimulates clearance  
65 mechanisms and facilitate entry into other cell types such as macrophages<sup>12,13</sup>.

66 The exposure of PS on the surface of apoptotic cells is a key “eat me” signal triggering  
67 engulfment by phagocytes<sup>10</sup>. Several PS receptors have been identified, including the T-cell  
68 immunoglobulin and mucin domain containing 4 (TIM-4) receptor, and anti-TIM-4 antibodies can  
69 block this engulfment process by macrophages<sup>14,15</sup>.

70 In this study, we developed novel chimeric engulfment receptors (CER) that take advantage of  
71 TIM-4 binding PS<sup>16</sup>. These CERs are composed of the extracellular TIM-4 domain and one or  
72 more intracellular signaling domains from receptors involved in innate immune responses to

73 pathogens; e.g., Toll-like receptors (TLR) <sup>17</sup>. Addition of innate immune function such as  
74 phagocytosis, antigen presentation, and greater lytic and non-cytolytic killing offers the potential  
75 of enhancing immune responses to chronic HIV infection. These CERs expressed in T cells  
76 provided the capability of eliminating simian immunodeficiency virus (SIV) infected cells in vitro.  
77 This investigation provides the initial rationale for use of CER T cells in in vivo models of  
78 nonhuman primate lentiviral infection to determine if the addition of functional killing and other  
79 innate functions such as enhanced antigen presentation and reversal of endogenous T helper  
80 responses can be improved through adoptive transfer experiments of T cells with enhanced  
81 engulfment function.

82

83

## 84 **RESULTS**

### 85 **TIM-4 binds to SIV infected CD4+ T cells**

86 Exposure of PS occurs when HIV infects CD4+ T cells <sup>11</sup>. To visualize TIM-4 binding to PS  
87 exposed on the surface of SIV infected cells, we created a fluorescent SIVmac239 virus <sup>18</sup>. The  
88 coding sequence for the enhanced green fluorescent protein (EGFP) was introduced between  
89 the matrix and capsid domains of the SIVmac239 Gag protein and flanked by SIV protease  
90 cleavage sites (SIVGAGGFP) (**Figure S1**).

91

92 To test if TIM-4 bound to SIV infected cells, we used a TIM-4 Fc chimera composed of the TIM-  
93 4 extracellular domain fused to the N-terminus of the human IgG Fc region. When CD4+ T cells  
94 were infected with SIVGAGGFP, strong binding of TIM-4 Fc to SIVGAGGFP+ cells was  
95 detected 1 hour post infection while no binding was observed on SIVGAGGFP- gated cells  
96 (**Figure 1A**). Binding of the labeled anti-IgG antibodies to SIVGAGGFP+ cells was not observed  
97 in the absence of TIM-4 incubation, thus confirming interaction of TIM-4 to SIV infected cells

98 **(Figure 1B)**. As a positive control, TIM-4 bound to cells undergoing apoptosis triggered by  
99 treatment with camptothecin **(Figure 1C)**.

100 The CCR5 coreceptor is necessary for SIV infection of CD4<sup>+</sup> T cells. CCR5 antagonist TAK-779  
101 blocks the interaction between CCR5 and SIV and inhibits PS exposure induced by R5-tropic  
102 virions <sup>11, 19, 20</sup>. Incubation of SIVGAGGFP with CD4<sup>+</sup> T cells in the presence of TAK-779  
103 decreased virion binding to target cells and also decreased TIM-4 binding to infected T cells  
104 **(Figure 1D)**. These results indicate that TIM-4 detects PS exposed on the surface of SIV  
105 infected cells.

#### 106 **CER T cells can kill SIV infected cells upon infection**

107 We initially constructed a series of prototype CER in order to evaluate if differences in signaling  
108 domains altered functional activity in vitro. All DNA constructs used the TIM-4 extracellular  
109 domain. As TLRs are known to enhance endosomal transfer and trafficking, some of the  
110 constructs tested contained a TLR signaling domain **(Figure 2A)**. The DNA constructs included  
111 a truncated version of the epidermal growth factor receptor (EGFR), which can be detected on  
112 the cell surface using an anti-EGFR monoclonal antibody, to assess the efficiency of lentiviral  
113 transduction into T cells. We also introduced a membrane anchored fusion inhibitory peptide  
114 derived from gp41 (C46) to protect the CD4<sup>+</sup> CER T cells against SIV infection <sup>21, 22</sup>. We first  
115 investigated if CD4<sup>+</sup> or CD8<sup>+</sup> CER T cells would be efficient in eliminating SIV infected T cells.  
116 Transduction of RM CD4<sup>+</sup> and CD8<sup>+</sup> T cells with CER21 or EGFR lentivirus led to high levels of  
117 EGFR expression **(Figure 2B)**. We developed a real-time fluorescence assay to evaluate CER  
118 T-cell potency against freshly SIVGFP infected target cells expressing surface-exposed PS <sup>23</sup>. A  
119 significant decrease in the number of GFP<sup>+</sup> infected T cells were detected over time in the  
120 presence of CD4<sup>+</sup> CER T cells but not CD8<sup>+</sup> CER T cells or EGFR T cells, indicating the  
121 potency of CD4 CER T cells in killing SIV-infected cells **(Figure 2C)**. To direct CER T cells to  
122 major sites of SIV/HIV persistence, the cDNA encoding RM CXCR5, a homing receptor shown

123 to promote cell trafficking to B-cell follicles in lymph nodes, was added to the lentiviral vector <sup>24-</sup>  
124 <sup>28</sup>. About 16% of the EGFR+ transduced T cells expressed both EGFR and CXCR5 (**Figure**  
125 **2D**). CD4+ CER T cells transduced with the CER21-CXCR5 lentivirus were efficient in killing  
126 SIV infected targets (**Figure 2E**).

### 127 **CER composed of a TLR8 signaling domain and CD3 $\zeta$ activation domain is the most** 128 **potent in killing SIV infected cells**

129 We designed 8 additional CERs by linking the extracellular domain of TIM-4 to various  
130 intracellular signaling domains with either the TIM-4 or CD28 transmembrane domain. The  
131 intracellular domain was composed of one or multiple engulfment signaling domains of TLR2,  
132 TLR8, tumor necrosis factor receptor associated factor 6 (TRAF6), DAP10, DAP12, and/or  
133 CD28. Some CERs also included TLR signaling domains together with the CD3 $\zeta$  activation  
134 domain (**Figure 3A**). High expression of the EGFR marker was observed for all 9 CER-  
135 transduced RM CD4+ T cells (**Figure 3B**). When comparing the effector functions of these CER  
136 T cells in the real-time fluorescence assay, we found diverse killing potency, with CER131  
137 (TLR8-CD3 $\zeta$ ) and CER29 (TRAF6) exhibiting the greatest effector functions towards SIV  
138 infected cells (**Figure 3C**).

### 139 **Mutations in the PS binding site of TIM-4 impair CER T-cell effector function**

140 In the immunoglobulin domain of TIM-4, a hydrophobic phenylalanine-glycine (FG) loop is  
141 located in a cavity important for metal ion interaction and PS binding <sup>29</sup>. Mutations of 4 amino  
142 acids, tryptophan, phenylalanine, asparagine and aspartic acid (WFND), present in this cavity  
143 result in loss of phagocytosis of apoptotic cells <sup>14</sup>. In order to determine whether CER effector  
144 functions are triggered upon specific recognition of PS by TIM-4, we generated CER constructs  
145 with alanine mutations or deletion of all 4 WFND residues (**Figure 4A**). After assessment of the  
146 transduction rate of CER T cells (**Figure 4B**), CER mutants were tested in the real-time killing

147 assay. Both mutants were impaired in their ability to eliminate SIV infected CD4+ T cells  
148 compared with wild-type CER131 (**Figure 4C**).

### 149 **Additive killing activity of CER T cells and anti-SIV CAR T cells against SIV infected cells**

150 As cytotoxic T-cell killing has been shown to elicit surface exposed PS on target cells, we  
151 evaluated potential additive effects between CER T cells and CAR T cells directed at SIV  
152 infected CD4+ T cells. For these experiments, we utilized two previously constructed lentivirus  
153 directed CAR T cells<sup>30</sup>. The first, ITS06, contains an scFv directed at the V1 region of SIV  
154 envelope and the second, VRC26, contains a V2 loop-directed scFv, which cross-reacts with  
155 HIV-1 in vitro and is representative of lower avidity but greater breadth. We evaluated  
156 combinations of CD4+ CER T cells with CD8+ and/or CD3+ anti-SIV CAR T cells in killing  
157 potency against SIV infected CD4+ RM cells. CD4+ CER T cells co-incubated with CD8+ ITS06  
158 CAR T cells induced additive killing of SIV infected target cells (**Figure 5A**). A dose response  
159 cytotoxic effect was observed using a E:T ratio of 5:1 for CER T cells and various E:T ratios of  
160 ITS06 CAR T cells; most readily seen at a low E:T ratio of 1:20 CAR T cells. A similar  
161 concentration dependent effect was seen in experiments using a combination of VRC26 CAR T  
162 cells with CER T cells (**Figure 5B**). These latter experiments used a 40-fold higher  
163 concentration of the VRC26 CAR T cells (E:T of 2:1) due to its reduced potency compared to  
164 ITS06 CAR T cells. These data suggest additive in vitro killing between CER and CAR T cells.

## 165 **DISCUSSION**

166 Although CAR T-cell therapies have shown some efficacy in controlling viral replication, anti-  
167 HIV/SIV CAR T cells have not reached the potential shown by CAR T cells targeting cancer  
168 cells. Some success in delaying and reducing SHIV or HIV viremia has been primarily achieved  
169 with CAR T cells based on the extracellular domain of the human CD4 receptor, while T cells  
170 expressing CARs engineered with the scFv of broadly neutralizing antibodies were not

171 successful likely because of anti-SIV antibodies blocking the interaction between the CAR scFv  
172 and its epitope <sup>22, 31-33</sup>. As such, development of novel chimeric receptors targeting different  
173 surface proteins and signaling through different immune pathways might lead to improved  
174 elimination of HIV infected cells.

175 Here, we investigated the potential of receptors triggering engulfment signals for the clearance  
176 of SIV infected cells. Phagocytes sense PS, the eat me signal, exposed at the surface of  
177 apoptotic T cells such as cancer or infected cells, which leads to phagocytic engulfment <sup>10</sup>.  
178 Although multiple PS receptors have been identified, TIM-4 has been shown to be necessary for  
179 apoptotic cell engulfment by macrophages <sup>14, 15</sup>. In this study, we demonstrated that TIM-4 can  
180 bind PS exposed on the surface of SIV infected cells and is thus a good candidate for  
181 engineering new receptors against SIV.

182 The TIM-4 PS binding protein in combination with other apoptotic cell clearance pathways led to  
183 a range of increased killing by the CER T cells. TLRs, a family of pattern recognition receptor  
184 proteins that recognize pathogen-associated molecular patterns and lead to activation of  
185 immune signaling pathways, have also been used to boost the immune response against  
186 cancer cells and tested as part of CAR T cells <sup>6, 34, 35</sup>. The TLR8 signaling pathway, including  
187 MyD88 and TRAF6, results in NF- $\kappa$ B expression and protection against RNA viruses <sup>36</sup>. DAP10  
188 and DAP12 are involved in kinase signaling cascades for a variety of immune response  
189 receptors <sup>37, 38</sup>. The CD28 costimulatory domain together with the CD3 $\zeta$  domain of the T-cell  
190 receptor triggers T-cell activation upon antigen recognition, and has been extensively used as  
191 signaling component of CAR T cells to promote cytokine production and cytotoxicity <sup>39, 40</sup>. We  
192 found that out of all the innate signaling constructs we tested, the TLR8-CD3 $\zeta$  combination and  
193 TRAF6 CER T cells killed target cells most efficiently. PS binding by TIM-4 on the surface of  
194 CER T cells was essential for killing and mutation in the PS binding pocket abolished activity.



195 The process triggered by the CER T cells to eliminate SIV infected cells has not been  
196 investigated. Prior studies suggest that killing by T cells engineered to express chimeric antigen  
197 receptors for phagocytosis (CAR-Ps) appears to be related to the cell's ability to nibble plasma  
198 membrane fragments of other target cells (i.e., trogocytosis)<sup>3, 41-43</sup>. CERs with diverse signaling  
199 domains provide new functionality to CD4+ T cells, and it is possible that different processes are  
200 triggered by each receptor<sup>16</sup>. For example, CER131 that includes a CD3 $\zeta$  activation domain  
201 might also trigger the activation of natural T-cell effector functions. Although no receptors similar  
202 to the CERs described in this study have been investigated and tested in T cells, CAR-Ps are  
203 another type of engulfment receptor composed of a specific scFv fused to intracellular signaling  
204 domains that contain immunoreceptor tyrosine-based activation motifs. These CAR-Ps when  
205 expressed in macrophages induce engulfment of specific targets, including cancer cells<sup>3, 44</sup>.  
206 However, for cell therapy, gene transfer into primary macrophages as well as manufacturing  
207 primary macrophages for infusion would likely be more complex and expensive than for T cells.  
208 While our data showing such an approach to eliminate SIV infected cells are provocative,  
209 several limitations exist. Whether SIV infected T cells are inhibited and put into endosomal  
210 pathways and "directed" are not yet known, although evidence for this has been seen with tumor  
211 cell lines<sup>16</sup>. Similarly, whether elimination is achieved by the CD4+, CD8+ or both populations of  
212 T cells remains to be determined. In ongoing experiments, most engulfment activity appears  
213 restricted to the CD4+ T-cell populations<sup>45</sup>. While a high safety profile has been shown in small  
214 animal models, whether off target effects will occur in NHP remains to be seen<sup>46</sup>.

215 In conclusion, we engineered novel types of chimeric receptors that provide CD4+ T cells the  
216 ability to eliminate SIV infected cells in vitro. These genetically engineered CER T cells  
217 enhanced in vitro cellular damage caused by high and low affinity CAR T cells, suggesting the  
218 approach could be evaluated in vivo. Lastly, in vivo studies will be required to define if the  
219 potency and ability of engulfment to enhance antigen presentation and endogenous immune

220 responses will occur in vivo with limited toxicity. To date, extensive animal model experiments in  
221 mice in tumor models have shown no evidence of hematologic or systemic toxicity<sup>45, 46</sup>.

222

## 223 **MATERIALS AND METHODS**

### 224 **Enrichment of CD4+ and CD8+ RM T lymphocytes**

225 Frozen peripheral blood mononuclear cells (PBMCs) from Indian genetic background RM  
226 (*Macaca mulatta*) were obtained from the Oregon National Primate Research Center in  
227 accordance with standards of the Center's Institutional Animal Care and Use Committee and  
228 the *National Institutes of Health Guide for the Care and Use of Laboratory Animals*.

229 Immunomagnetic negative selection (Easy Sep NHP, STEMCELL Technologies, Cambridge,  
230 MA) was used to enrich in CD4+ or CD8+ T cells from PBMCs that were cultured in X-vivo 15  
231 media (Lonza) supplemented with 10% FBS, 100 U/ml Pen/Strep, 1 x glutamax and 50 IU/ml  
232 human recombinant IL-2 (Peprotech, Cranbury, NJ). Enriched CD4+ and CD8+ T cells were  
233 activated with ImmunoCult NHP CD2/CD3/CD28 T-cell activator (STEMCELL Technologies)  
234 and incubated 3 days at 37°C in humidified 5% CO<sub>2</sub>.

235

### 236 **Production of SIVGAGGFP and SIVGFP and CD4 T-cell infection**

237 To generate the fluorescent SIVmac239 virus (SIVGAGGFP), we introduced cDNA encoding  
238 enhanced green fluorescent protein (EGFP) together with protease cleavage sites and  
239 restriction sites between the matrix and capsid domains of Gag of the full-length  
240 SIV<sub>MAC239</sub> proviral DNA using PCR and the NEBuilder HiFi DNA Assembly (New England  
241 Biolabs, Ipswich, MA) and used the same strategy as Hubner et al to generate the HIV Gag-  
242 iGFP<sup>18</sup>. The junction between MA and EGFP is as follows: 5'-

243 CCATCTAGCGGCAGAGGAGGAAATTACCCAGTACAACAAACGCGTATGGCTAGCAAGGGC

244 -3' where the MA coding sequence is underlined, the protease cleavage site is in italics, the *MluI*

245 restriction site is in underlined italics and followed by the EGFP sequence. The junction between  
246 EGFP and CA is as follows: 5'-  
247 GACGAGCTGTACAAG TCTAGAGGAGGAAATTACCCAGTACAACAAATAGGTGGTAACTAT-  
248 3' where the EGFP coding sequence is followed by the *Xba*I restriction site in underlined italics,  
249 the protease cleavage site in italics and the underlined CA coding sequence. Virus production  
250 for SIVGAGGFP and SIVGFP, a recombinant SIVmac239 virus with an IRES-EGFP cassette  
251 downstream of the *nef* gene illustrated in our previous work, was performed as previously  
252 described <sup>23</sup>. Briefly, HEK293T cells were transfected with 20 µg of the SIVGAGGFP or SIVGFP  
253 plasmid using the calcium phosphate method. The fluorescent viral supernatant was collected  
254 48 hours later, cleared by centrifugation, filtered, and concentrated. Stocks of SIVGAGGFP or  
255 SIVGFP viruses were titrated using TZM-bl cells as described by Wei et al <sup>47</sup>. Infection of CD4  
256 targets was performed by adding ~ 20µl of concentrated fluorescent SIV viruses to 10<sup>5</sup> CD4  
257 cells (MOI:0.5) or control Jurkat 76 cells <sup>48</sup> plated on retronectin-coated 96-well plates followed  
258 by spinoculation for 2 hours at 1,200 x g. The SIV-infected cells were assessed for infection  
259 using flow cytometry after gating on lymphocytes and single cells.

260

#### 261 **TIM-4 binding assays**

262 Binding of TIM-4 to infected cells was tested using a TIM-4 Fc chimera composed of the  
263 extracellular domain of TIM-4 fused to the N-terminus of the Fc region of human IgG (Abcam,  
264 Waltham, MA). One µg of TIM-4 in PBS containing 1% BSA was incubated on ice for 30  
265 minutes with 10<sup>5</sup> washed CD4 T cells infected as indicated above with SIVGAGGFP. After  
266 washing, the cells were incubated for 15 minutes on ice with an Alexa Fluor 647-anti-IgG  
267 antibody (clone M1301G05, Biolegend, San Diego, CA). Control experiments were performed  
268 by skipping the incubation with TIM-4. Binding of TIM-4 to SIVGAGGFP infected cells was  
269 analyzed by flow cytometry after gating on lymphocytes, single cells and GFP+ cells. When

270 indicated, the CD4 T cells were incubated with 10  $\mu$ m TAK-779 (Medchemexpress, Monmouth  
271 Junction, NJ) for 15 minutes before adding the SIVGAGGFP virus and infection of cells. Control  
272 apoptotic cells were prepared by incubating CD4 T cells with 2  $\mu$ M camptothecin (Sigma-  
273 Aldrich, St. Louis, MO) overnight at 37°C.

#### 274 **Generation of lentiviral transfer plasmids and transduction into RM T cells**

275 All CER constructs were generated by standard PCR cloning techniques and the PCR products  
276 were assembled using the NEBuilder HiFi DNA Assembly (New England Biolabs). CER21 was  
277 generated by linking the extracellular and transmembrane domain of human TIM-4 (GenBank™  
278 accession number AAH08988.1, residues 1 to 335) with the signaling domain of the human toll-  
279 like receptor 8 (TLR8) (GenBank™ accession number AAQ88663.1, residues 849 to 1041). The  
280 CER are fused to a truncated EGFR as a marker to identify transduced cells via a Thosa  
281 asigna virus 2A (T2A) self-cleavage peptide. The C46 inhibitory peptide preceded by a T2A self-  
282 cleavage peptide and a signal peptide and linked through an IgG2 hinge to the membrane  
283 spanning domain of CD34<sup>49</sup> was also added as a PCR product to the CER construct. When  
284 indicated, a cDNA encoding the rhesus CXCR5 (Sino Biological, GenBank™ accession number  
285 XP\_001100017.2) preceded by a porcine teschovirus-1 2A (P2A) cleavage site was also added  
286 downstream of the C46 to build the CER-CXCR5. Control EGFR and EGFR-CXCR5 were  
287 generated by removing the CER from the above construct using the NEBuilder HiFi DNA  
288 Assembly (New England Biolabs). CER 104 and CER 131 were generated by adding the human  
289 DAP 12 signaling domain (GenBank™ accession number NP\_001166985, residues 51 to 102)  
290 or the human CD3z activation domain (GenBank™ accession number NP\_932170.1, residues  
291 52 to 164), respectively, downstream of the TLR8 domain in CER21. CER132 was constructed  
292 by adding the human DAP 10 signaling domain (GenBank™ accession number NP\_055081,  
293 residues 70-93) downstream of the TLR8 and DAP12 signaling domains in CER104. The CER  
294 133 is composed of the human TLR2 signaling domain (GenBank™ accession number

295 AAY85648, residues 610 to 784) and CD3z activation domain. CER 129 is composed of the  
296 signaling domain of the human TNF receptor-associated factor 6 (TRAF6) (GenBank™  
297 accession number AAH31052, residues 1 to 274). CER140 and CER137 were generated by  
298 linking the extracellular domain of TIM-4 (GenBank™ accession number AAH08988.1 residues  
299 1 to 314) to the transmembrane domain and signaling domain of human CD28 with or without  
300 the CD28 hinge, respectively (GenBank™ accession number NP\_006130.1, residues 114 to  
301 220 (with hinge) or residues 153 to 220 (without hinge)). These CER or control EGFR constructs  
302 were cloned together with a woodchuck hepatitis virus posttranscriptional regulatory element  
303 (WPRE) into a SIV-based lentiviral vector (a generous gift from Dr. Nienhuis, St June Children's  
304 Research hospital, Memphis, TN and Dr. Miyazaki, Osaka University, Japan)<sup>50, 51</sup>. The  
305 production of recombinant lentiviruses was performed as previously described<sup>23</sup>. Briefly, Lenti-  
306 XTM 293T cells (Takara Bio) in DMEM media containing 10% FBS and 100 U/ml Pen/Strep  
307 were transfected using the standard calcium phosphate method with 15 µg of the CER transfer  
308 vector, 6 µg of the pCAG-SIVgprre (*gag/pol* and *rev* responsive element [RRE]), 4 µg of the  
309 *rev/tat* expression plasmid pCAG4-RTR-SIV and 3 µg of the pMD2.CocalG (glycoprotein G of  
310 the cocal virus)<sup>52</sup>. After overnight incubation, cells were washed and added fresh media. One  
311 and 2 days later, lentivirus-containing media was collected, cleared by centrifugation at 1,000 x  
312 g for 5 minutes followed by filtration on a 0.45 µm Millipore filter, and concentrated (50 X) by  
313 ultracentrifugation at 74,000xg for 2 hours at 4°C. The lentivirus stocks were titrated by  
314 transduction of Jurkat cells cultured in RPMI media supplemented with 10% FBS and 100 U/ml  
315 Pen/Strep using spinoculation for 2 hours at 1,200xg. The percentage of transduced Jurkat cells  
316 was quantified by flow analysis for EGFR using the anti-EGFR cetuximab mAb (Erbix, PE-  
317 conjugated at Juno Therapeutics, Seattle, WA).

318 For the transduction of CD4+ or CD8+ T cells, cells were mixed on retronectin (Takara Bio)-  
319 coated plates with CER lentivirus at a MOI of ~ 20 followed by spinoculation for 2 hours at

320 1,200xg. Cells were washed about 24 hours after transduction and expanded in fresh complete  
321 X-vivo 15 media. Four days after transduction, T cells were analyzed for EGFR expression by  
322 flow cytometry using PE-anti-EGFR, BV421 anti-CD4 (OKT4, Biolegend) and APC-Cyanine7  
323 anti-CD8 (SK1, Biolegend). EGFR expression was analyzed using FlowJo and sequential gating  
324 on lymphocytes, single cells and then CD4+ or CD8+ T cells.

### 325 **Real-time monitoring of cell infection to assess CER T-cell potency in eliminating SIV-** 326 **infected CD4**

327 The targets were prepared at the time of the assay. A master mix was prepared by adding  
328 SIVGFP at a MOI of ~ 0.5 to 4.  $10^5$  CD4 T cells/ml. Fifty  $\mu$ l/well of the mix (20,000 CD4 T cells +  
329 SIVGFP) were distributed into BioCoat poly-D-lysine coated flat bottom 96-well plate and  
330 spinoculated. CER T cells or control cells were then added at the effector:target (E:T ratio) of  
331 5:1 in triplicate wells. Plates were incubated at 37°C in the IncuCyte S3 LiveCell Analysis  
332 System (Sartorius) and five images of each well were recorded every 3 hours and analyzed with  
333 the IncuCyte image analysis software to determine the number of infected cells becoming  
334 fluorescent overtime.

335

### 336 **ITS06 CAR T-cell preparation**

337 The design and assembly of the ITS06 CAR and VRC26 CAR was previously described<sup>30</sup>. The  
338 ITS06 CAR was composed to the ITS06 scFv in a VH-VL orientation and a medium spacer of  
339 119 amino acids linked to a CD28 transmembrane domain, a 4-1BB intracellular costimulatory  
340 domain, and a CD3z activation domain and was also fused via a T2A peptide to a truncated  
341 EGFR as a marker to identify transduced cells. The VRC26 CAR vector consisted of the scFv of  
342 the VRC26.25 bnAb and a short spacer of 12 amino acids linked to a CD28 transmembrane  
343 domain, a 4-1BB intracellular costimulatory domain, and a CD3z activation domain and fused to

344 a truncated EGFR via a T2A peptide. Both the ITS06 CAR and the VRC26 CAR were also  
345 fused to a T2A-C46-peptide-P2A-CXCR5 cassette as described above for the CER vector. The  
346 production of recombinant lentiviruses for the CAR and the transduction of T lymphocytes with  
347 the CAR lentiviruses was performed as described above for the preparation of the CER T cells.  
348 Transduction efficiency was determined by flow cytometry analysis using PE-anti-EGFR.

349

### 350 **Real-time assay to assess the additive effect of CER T cells and CAR T cells against SIV-** 351 **infected cells**

352 The real time assay to monitor infection of RM CD4 T cells was performed as described above  
353 except that instead of CER T cells, a mix of CER T cells at a fixed ratio (E:T of 5:1) and various  
354 amounts of CAR T cells as indicated in the figures were added together to the SIV-infected  
355 targets.

356

### 357 **Statistics**

358 Data of the real time assays are presented as the mean  $\pm$  standard error of the mean. Statistical  
359 significance was analyzed by Student's t test at time indicated in the figure legend and  
360 compared to controls.

361

### 362 **ACKNOWLEDGEMENTS**

363 Our studies were funded by the Gilead Foundation and NIH/NIAID (grant UM1AI126623-05).  
364 We thank Dr. Arthur Nienhuis (St June Children's Research hospital, Memphis, TN, US) and Dr.  
365 Jun-ichi Miyazaki (Osaka University, Japan) for kindly providing the SIV-based lentiviral vectors  
366 <sup>50, 51</sup> and Drs. Serge Barcy, Mindy Miner and Karsten Eichholz for suggestions, critiques and  
367 editing of the manuscript. DC has filed patents on the development of CER T cells, which are

368 licensed to Cero Therapeutics; he is employed by Cero Therapeutics. LC is on the Scientific  
369 Advisory Board of Cero Therapeutics. FH declares no conflicts of interest.

370

## 371 **AUTHOR CONTRIBUTIONS**

372 Co-first authorship is listed alphabetically. DC conceived the idea of using TIM-4 and designed  
373 the CER T cells including in vitro screens for engulfment activity for the lead constructs. FH  
374 designed and performed all the in vitro experiments and wrote the first draft of the manuscript.  
375 LC planned the studies and collaboration. FH and LC had unrestricted access to all data. All  
376 authors agreed to submit the manuscript, read and approved the final draft and take full  
377 responsibility of its content.

378

379

380

381

382

383

384

385

386

387

388



## 389 REFERENCES

- 390 1. Gill S, Maus MV, Porter DL. Chimeric antigen receptor T cell therapy: 25years in the making.  
391 Blood Rev. 2016;30(3):157-67. Epub 2015/11/18. doi: 10.1016/j.blre.2015.10.003. PubMed PMID:  
392 26574053.
- 393 2. Maus MV, Grupp SA, Porter DL, June CH. Antibody-modified T cells: CARs take the front seat for  
394 hematologic malignancies. Blood. 2014;123(17):2625-35. Epub 2014/03/01. doi: 10.1182/blood-2013-  
395 11-492231. PubMed PMID: 24578504; PMCID: PMC3999751.
- 396 3. Morrissey MA, Williamson AP, Steinbach AM, Roberts EW, Kern N, Headley MB, Vale RD.  
397 Chimeric antigen receptors that trigger phagocytosis. Elife. 2018;7. Epub 2018/06/05. doi:  
398 10.7554/eLife.36688. PubMed PMID: 29862966; PMCID: PMC6008046.
- 399 4. Britt EA, Gitau V, Saha A, Williamson AP. Modular Organization of Engulfment Receptors and  
400 Proximal Signaling Networks: Avenues to Reprogram Phagocytosis. Front Immunol. 2021;12:661974.  
401 Epub 2021/05/07. doi: 10.3389/fimmu.2021.661974. PubMed PMID: 33953723; PMCID: PMC8092387.
- 402 5. Töpfer K, Cartellieri M, Michen S, Wiedemuth R, Müller N, Lindemann D, Bachmann M, Füssel M,  
403 Schackert G, Temme A. DAP12-based activating chimeric antigen receptor for NK cell tumor  
404 immunotherapy. J Immunol. 2015;194(7):3201-12. Epub 2015/03/06. doi: 10.4049/jimmunol.1400330.  
405 PubMed PMID: 25740942.
- 406 6. Pahlavanneshan S, Sayadmanesh A, Ebrahimiyan H, Basiri M. Toll-Like Receptor-Based Strategies  
407 for Cancer Immunotherapy. J Immunol Res. 2021;2021:9912188. Epub 2021/06/15. doi:  
408 10.1155/2021/9912188. PubMed PMID: 34124272; PMCID: PMC8166496 of this paper.
- 409 7. Chun TW, Stuyver L, Mizell SB, Ehler LA, Mican JA, Baseler M, Lloyd AL, Nowak MA, Fauci AS.  
410 Presence of an inducible HIV-1 latent reservoir during highly active antiretroviral therapy. Proc Natl Acad  
411 Sci U S A. 1997;94(24):13193-7. Epub 1997/12/16. doi: 10.1073/pnas.94.24.13193. PubMed PMID:  
412 9371822; PMCID: PMC24285.
- 413 8. Siliciano JD, Kajdas J, Finzi D, Quinn TC, Chadwick K, Margolick JB, Kovacs C, Gange SJ, Siliciano  
414 RF. Long-term follow-up studies confirm the stability of the latent reservoir for HIV-1 in resting CD4+ T  
415 cells. Nat Med. 2003;9(6):727-8. Epub 2003/05/20. doi: 10.1038/nm880. PubMed PMID: 12754504.
- 416 9. Estes JD, Kityo C, Ssali F, Swainson L, Makamdop KN, Del Prete GQ, Deeks SG, Luciw PA, Chipman  
417 JG, Beilman GJ, Hoskuldsson T, Khoruts A, Anderson J, Deleage C, Jasurda J, Schmidt TE, Hafertepe M,  
418 Callisto SP, Pearson H, Reimann T, Schuster J, Schoephoerster J, Southern P, Perkey K, Shang L,  
419 Wietgreffe SW, Fletcher CV, Lifson JD, Douek DC, McCune JM, Haase AT, Schacker TW. Defining total-  
420 body AIDS-virus burden with implications for curative strategies. Nat Med. 2017;23(11):1271-6. Epub  
421 2017/10/03. doi: 10.1038/nm.4411. PubMed PMID: 28967921; PMCID: PMC5831193.
- 422 10. Park SY, Kim IS. Engulfment signals and the phagocytic machinery for apoptotic cell clearance.  
423 Exp Mol Med. 2017;49(5):e331. Epub 2017/05/13. doi: 10.1038/emm.2017.52. PubMed PMID:  
424 28496201; PMCID: PMC5454446.
- 425 11. Zaitseva E, Zaitsev E, Melikov K, Arakelyan A, Marin M, Villasmil R, Margolis LB, Melikyan GB,  
426 Chernomordik LV. Fusion Stage of HIV-1 Entry Depends on Virus-Induced Cell Surface Exposure of  
427 Phosphatidylserine. Cell Host Microbe. 2017;22(1):99-110.e7. Epub 2017/07/14. doi:  
428 10.1016/j.chom.2017.06.012. PubMed PMID: 28704658; PMCID: PMC5558241.
- 429 12. Chua BA, Ngo JA, Situ K, Morizono K. Roles of phosphatidylserine exposed on the viral envelope  
430 and cell membrane in HIV-1 replication. Cell Commun Signal. 2019;17(1):132. Epub 2019/10/23. doi:  
431 10.1186/s12964-019-0452-1. PubMed PMID: 31638994; PMCID: PMC6805584.
- 432 13. Callahan MK, Popernack PM, Tsutsui S, Truong L, Schlegel RA, Henderson AJ. Phosphatidylserine  
433 on HIV envelope is a cofactor for infection of monocytic cells. J Immunol. 2003;170(9):4840-5. Epub  
434 2003/04/23. doi: 10.4049/jimmunol.170.9.4840. PubMed PMID: 12707367.

- 435 14. Kobayashi N, Karisola P, Peña-Cruz V, Dorfman DM, Jinushi M, Umetsu SE, Butte MJ, Nagumo H,  
436 Chernova I, Zhu B, Sharpe AH, Ito S, Dranoff G, Kaplan GG, Casasnovas JM, Umetsu DT, Dekruyff RH,  
437 Freeman GJ. TIM-1 and TIM-4 glycoproteins bind phosphatidylserine and mediate uptake of apoptotic  
438 cells. *Immunity*. 2007;27(6):927-40. Epub 2007/12/18. doi: 10.1016/j.immuni.2007.11.011. PubMed  
439 PMID: 18082433; PMCID: PMC2757006.
- 440 15. Miyanishi M, Tada K, Koike M, Uchiyama Y, Kitamura T, Nagata S. Identification of Tim4 as a  
441 phosphatidylserine receptor. *Nature*. 2007;450(7168):435-9. Epub 2007/10/26. doi:  
442 10.1038/nature06307. PubMed PMID: 17960135.
- 443 16. Corey D, inventor Chimeric engulfment receptor molecules and methods of use. USA patent  
444 WO2019067328A1. 2019 April 4, 2019.
- 445 17. Fitzgerald KA, Kagan JC. Toll-like Receptors and the Control of Immunity. *Cell*. 2020;180(6):1044-  
446 66. Epub 2020/03/14. doi: 10.1016/j.cell.2020.02.041. PubMed PMID: 32164908.
- 447 18. Hübner W, Chen P, Del Portillo A, Liu Y, Gordon RE, Chen BK. Sequence of human  
448 immunodeficiency virus type 1 (HIV-1) Gag localization and oligomerization monitored with live confocal  
449 imaging of a replication-competent, fluorescently tagged HIV-1. *J Virol*. 2007;81(22):12596-607. Epub  
450 2007/08/31. doi: 10.1128/jvi.01088-07. PubMed PMID: 17728233; PMCID: PMC2168995.
- 451 19. Baba M, Nishimura O, Kanzaki N, Okamoto M, Sawada H, Iizawa Y, Shiraishi M, Aramaki Y,  
452 Okonogi K, Ogawa Y, Meguro K, Fujino M. A small-molecule, nonpeptide CCR5 antagonist with highly  
453 potent and selective anti-HIV-1 activity. *Proc Natl Acad Sci U S A*. 1999;96(10):5698-703. Epub  
454 1999/05/13. doi: 10.1073/pnas.96.10.5698. PubMed PMID: 10318947; PMCID: PMC21923.
- 455 20. Sougrat R, Bartesaghi A, Lifson JD, Bennett AE, Bess JW, Zabransky DJ, Subramaniam S. Electron  
456 tomography of the contact between T cells and SIV/HIV-1: implications for viral entry. *PLoS Pathog*.  
457 2007;3(5):e63. Epub 2007/05/08. doi: 10.1371/journal.ppat.0030063. PubMed PMID: 17480119; PMCID:  
458 PMC1864992.
- 459 21. Egelhofer M, Brandenburg G, Martinius H, Schult-Dietrich P, Melikyan G, Kunert R, Baum C, Choi  
460 I, Alexandrov A, von Laer D. Inhibition of human immunodeficiency virus type 1 entry in cells expressing  
461 gp41-derived peptides. *J Virol*. 2004;78(2):568-75. Epub 2003/12/25. doi: 10.1128/jvi.78.2.568-  
462 575.2004. PubMed PMID: 14694088; PMCID: PMC368739.
- 463 22. Françoise Haeseleer YF, Haesun Park, Benjamin Varco-Merth, Blake J. Rust, Jeremy V. Smedley,  
464 Karsten Eichholz, Christopher W. Peterson, Rosemarie Mason, Hans-Peter Kiem, Mario Roederer, Louis J.  
465 Picker, Afam A. Okoye, Lawrence Corey. Immune inactivation of anti-simian immunodeficiency virus  
466 chimeric antigen receptor T cells in rhesus macaques. *Molecular Therapy- Methods & Clinical*  
467 *Development*. 2021.
- 468 23. Haeseleer F, Eichholz K, Tareen SU, Iwamoto N, Roederer M, Kirchhoff F, Park H, Okoye AA,  
469 Corey L. Real-Time Killing Assays to Assess the Potency of a New Anti-Simian Immunodeficiency Virus  
470 Chimeric Antigen Receptor T Cell. *AIDS Res Hum Retroviruses*. 2020. Epub 2020/09/30. doi:  
471 10.1089/aid.2020.0163. PubMed PMID: 32988211.
- 472 24. Fukazawa Y, Lum R, Okoye AA, Park H, Matsuda K, Bae JY, Hagen SI, Shoemaker R, Deleage C,  
473 Lucero C, Morcock D, Swanson T, Legasse AW, Axthelm MK, Hesselgesser J, Geleziunas R, Hirsch VM,  
474 Edlefsen PT, Piatak M, Jr., Estes JD, Lifson JD, Picker LJ. B cell follicle sanctuary permits persistent  
475 productive simian immunodeficiency virus infection in elite controllers. *Nat Med*. 2015;21(2):132-9.  
476 Epub 2015/01/20. doi: 10.1038/nm.3781. PubMed PMID: 25599132; PMCID: PMC4320022.
- 477 25. Banga R, Procopio FA, Noto A, Pollakis G, Cavassini M, Ohmiti K, Corpataux JM, de Leval L,  
478 Pantaleo G, Perreau M. PD-1(+) and follicular helper T cells are responsible for persistent HIV-1  
479 transcription in treated aviremic individuals. *Nat Med*. 2016;22(7):754-61. Epub 2016/05/31. doi:  
480 10.1038/nm.4113. PubMed PMID: 27239760.

- 481 26. Bronnimann MP, Skinner PJ, Connick E. The B-Cell Follicle in HIV Infection: Barrier to a Cure.  
482 *Front Immunol.* 2018;9:20. Epub 2018/02/10. doi: 10.3389/fimmu.2018.00020. PubMed PMID:  
483 29422894; PMCID: PMC5788973.
- 484 27. Haran KP, Hajduczki A, Pampusch MS, Mwakalundwa G, Vargas-Inchaustegui DA, Rakasz EG,  
485 Connick E, Berger EA, Skinner PJ. Simian Immunodeficiency Virus (SIV)-Specific Chimeric Antigen  
486 Receptor-T Cells Engineered to Target B Cell Follicles and Suppress SIV Replication. *Front Immunol.*  
487 2018;9:492. Epub 2018/04/05. doi: 10.3389/fimmu.2018.00492. PubMed PMID: 29616024; PMCID:  
488 PMC5869724.
- 489 28. Connick E, Folkvord JM, Lind KT, Rakasz EG, Miles B, Wilson NA, Santiago ML, Schmitt K,  
490 Stephens EB, Kim HO, Wagstaff R, Li S, Abdelaal HM, Kemp N, Watkins DI, MaWhinney S, Skinner PJ.  
491 Compartmentalization of simian immunodeficiency virus replication within secondary lymphoid tissues  
492 of rhesus macaques is linked to disease stage and inversely related to localization of virus-specific CTL. *J*  
493 *Immunol.* 2014;193(11):5613-25. Epub 2014/11/02. doi: 10.4049/jimmunol.1401161. PubMed PMID:  
494 25362178; PMCID: PMC4239212.
- 495 29. Santiago C, Ballesteros A, Martínez-Muñoz L, Mellado M, Kaplan GG, Freeman GJ, Casasnovas  
496 JM. Structures of T cell immunoglobulin mucin protein 4 show a metal-ion-dependent ligand binding site  
497 where phosphatidylserine binds. *Immunity.* 2007;27(6):941-51. Epub 2007/12/18. doi:  
498 10.1016/j.immuni.2007.11.008. PubMed PMID: 18083575; PMCID: PMC2330274.
- 499 30. Haeseleer F, Fukazawa Y, Park H, Varco-Merth B, Rust BJ, Smedley JV, Eichholz K, Peterson CW,  
500 Mason R, Kiem HP, Roederer M, Picker LJ, Okoye AA, Corey L. Immune inactivation of anti-simian  
501 immunodeficiency virus chimeric antigen receptor T cells in rhesus macaques. *Mol Ther Methods Clin*  
502 *Dev.* 2021;22:304-19. Epub 2021/09/07. doi: 10.1016/j.omtm.2021.06.008. PubMed PMID: 34485613;  
503 PMCID: PMC8403686.
- 504 31. Leibman RS, Richardson MW, Ellebrecht CT, Maldini CR, Glover JA, Secreto AJ, Kulikovskaya I,  
505 Lacey SF, Akkina SR, Yi Y, Shaheen F, Wang J, Dufendach KA, Holmes MC, Collman RG, Payne AS, Riley JL.  
506 Supraphysiologic control over HIV-1 replication mediated by CD8 T cells expressing a re-engineered CD4-  
507 based chimeric antigen receptor. *PLoS Pathog.* 2017;13(10):e1006613. Epub 2017/10/13. doi:  
508 10.1371/journal.ppat.1006613. PubMed PMID: 29023549; PMCID: PMC5638568 following competing  
509 interests: RSL, CTE, ASP, and JLR have filed a patent describing the construction of these HIV specific  
510 CARs. MCH and JW are employees of Sangamo Biosciences JLR cofounded a company called Tmunity  
511 Therapeutics that has the rights to license the technology describe in this paper. JLR holds an equity  
512 interest in Tmunity.
- 513 32. Rust BJ, Kean LS, Colonna L, Brandenstein KE, Poole NH, Obenza W, Enstrom MR, Maldini CR,  
514 Ellis GI, Fennessey CM, Huang ML, Keele BF, Jerome KR, Riley JL, Kiem HP, Peterson CW. Robust  
515 expansion of HIV CAR T cells following antigen boosting in ART-suppressed nonhuman primates. *Blood.*  
516 2020;136(15):1722-34. Epub 2020/07/03. doi: 10.1182/blood.2020006372. PubMed PMID: 32614969;  
517 PMCID: PMC7544543 Therapeutics that has the rights to license the technology described in this paper;  
518 and he holds an equity interest in Tmunity. The remaining authors declare no competing financial  
519 interests.
- 520 33. Iwamoto N, Patel B, Song K, Mason R, Bolivar-Wagers S, Bergamaschi C, Pavlakis GN, Berger E,  
521 Roederer M. Evaluation of chimeric antigen receptor T cell therapy in non-human primates infected with  
522 SHIV or SIV. *PLoS One.* 2021;16(3):e0248973. Epub 2021/03/23. doi: 10.1371/journal.pone.0248973.  
523 PubMed PMID: 33752225; PMCID: PMC7984852.
- 524 34. Lai Y, Weng J, Wei X, Qin L, Lai P, Zhao R, Jiang Z, Li B, Lin S, Wang S, Wu Q, Tang Z, Liu P, Pei D,  
525 Yao Y, Du X, Li P. Toll-like receptor 2 costimulation potentiates the antitumor efficacy of CAR T Cells.  
526 *Leukemia.* 2018;32(3):801-8. Epub 2017/08/26. doi: 10.1038/leu.2017.249. PubMed PMID: 28841215.
- 527 35. Caron G, Duluc D, Frémaux I, Jeannin P, David C, Gascan H, Delneste Y. Direct stimulation of  
528 human T cells via TLR5 and TLR7/8: flagellin and R-848 up-regulate proliferation and IFN-gamma

- 529 production by memory CD4+ T cells. *J Immunol.* 2005;175(3):1551-7. Epub 2005/07/22. doi:  
530 10.4049/jimmunol.175.3.1551. PubMed PMID: 16034093.
- 531 36. Konno H, Yamamoto T, Yamazaki K, Gohda J, Akiyama T, Semba K, Goto H, Kato A, Yujiri T, Imai  
532 T, Kawaguchi Y, Su B, Takeuchi O, Akira S, Tsunetsugu-Yokota Y, Inoue J. TRAF6 establishes innate  
533 immune responses by activating NF-kappaB and IRF7 upon sensing cytosolic viral RNA and DNA. *PLoS*  
534 *One.* 2009;4(5):e5674. Epub 2009/05/30. doi: 10.1371/journal.pone.0005674. PubMed PMID:  
535 19479062; PMCID: PMC2682567.
- 536 37. Lanier LL. DAP10- and DAP12-associated receptors in innate immunity. *Immunol Rev.*  
537 2009;227(1):150-60. Epub 2009/01/06. doi: 10.1111/j.1600-065X.2008.00720.x. PubMed PMID:  
538 19120482; PMCID: PMC2794881.
- 539 38. Orr MT, Sun JC, Hesslein DG, Arase H, Phillips JH, Takai T, Lanier LL. Ly49H signaling through  
540 DAP10 is essential for optimal natural killer cell responses to mouse cytomegalovirus infection. *J Exp*  
541 *Med.* 2009;206(4):807-17. Epub 2009/04/01. doi: 10.1084/jem.20090168. PubMed PMID: 19332875;  
542 PMCID: PMC2715124.
- 543 39. Jensen M, Tan G, Forman S, Wu AM, Raubitschek A. CD20 is a molecular target for scFvFc:zeta  
544 receptor redirected T cells: implications for cellular immunotherapy of CD20+ malignancy. *Biol Blood*  
545 *Marrow Transplant.* 1998;4(2):75-83. Epub 1998/10/08. doi: 10.1053/bbmt.1998.v4.pm9763110.  
546 PubMed PMID: 9763110.
- 547 40. Gill S, June CH. Going viral: chimeric antigen receptor T-cell therapy for hematological  
548 malignancies. *Immunol Rev.* 2015;263(1):68-89. Epub 2014/12/17. doi: 10.1111/imr.12243. PubMed  
549 PMID: 25510272.
- 550 41. Joly E, Hudrisier D. What is trogocytosis and what is its purpose? *Nat Immunol.* 2003;4(9):815.  
551 Epub 2003/08/28. doi: 10.1038/ni0903-815. PubMed PMID: 12942076.
- 552 42. Jim Reed MRaSAW. Lymphocytes and Trogocytosis-Mediated Signaling. *Cells.* 2021;10(6):18.
- 553 43. Reed J, Wetzel SA. Trogocytosis-Mediated Intracellular Signaling in CD4(+) T Cells Drives T(H)2-  
554 Associated Effector Cytokine Production and Differentiation. *J Immunol.* 2019;202(10):2873-87. Epub  
555 2019/04/10. doi: 10.4049/jimmunol.1801577. PubMed PMID: 30962293; PMCID: PMC6504583.
- 556 44. Klichinsky M, Ruella M, Shestova O, Lu XM, Best A, Zeeman M, Schmierer M, Gabrusiewicz K,  
557 Anderson NR, Petty NE, Cummins KD, Shen F, Shan X, Veliz K, Blouch K, Yashiro-Ohtani Y, Kenderian SS,  
558 Kim MY, O'Connor RS, Wallace SR, Kozlowski MS, Marchione DM, Shestov M, Garcia BA, June CH, Gill S.  
559 Human chimeric antigen receptor macrophages for cancer immunotherapy. *Nat Biotechnol.*  
560 2020;38(8):947-53. Epub 2020/05/04. doi: 10.1038/s41587-020-0462-y. PubMed PMID: 32361713;  
561 PMCID: PMC7883632.
- 562 45. Cieniewicz B, Nguyen L, Thomas S, Torabi D, Kethar H, Bobbin M, Bhatta A, Corey D, editors.  
563 Tim-4-Chimeric Engulfment Receptor (CER) T-cell Therapy Elicits Phosphatidylserine-Dependent  
564 Cytotoxic and Antigen-presenting Cell-like Function and Synergizes with Approved BTK Inhibitors for the  
565 Treatment of Hematologic Malignancies. *ASGCT; 2022; Washington, DC, USA.*
- 566 46. Bobbin M, Bhatia A, Eid R, Thomas S, Ning H, Clever J, Fragozo F, Kethar H, Rossi J, Cieniewicz B,  
567 Corey D, editors. Tim-4-Chimeric Engulfment Receptor (CER) T Cells Elicit Phosphatidylserine-Dependent  
568 Cytotoxic and Innate-Like Function and Synergizes with Approved PARP Inhibitors in an Ovarian Cancer  
569 Model. *ASTGCT; 2022; Washington, DC, USA.*
- 570 47. Wei X, Decker JM, Liu H, Zhang Z, Arani RB, Kilby JM, Saag MS, Wu X, Shaw GM, Kappes JC.  
571 Emergence of resistant human immunodeficiency virus type 1 in patients receiving fusion inhibitor (T-  
572 20) monotherapy. *Antimicrob Agents Chemother.* 2002;46(6):1896-905. Epub 2002/05/23. doi:  
573 10.1128/aac.46.6.1896-1905.2002. PubMed PMID: 12019106; PMCID: PMC127242.
- 574 48. Heemskerk MH, Hoogeboom M, de Paus RA, Kester MG, van der Hoorn MA, Goulmy E, Willemze  
575 R, Falkenburg JH. Redirection of antileukemic reactivity of peripheral T lymphocytes using gene transfer  
576 of minor histocompatibility antigen HA-2-specific T-cell receptor complexes expressing a conserved

577 alpha joining region. *Blood*. 2003;102(10):3530-40. Epub 2003/07/19. doi: 10.1182/blood-2003-05-1524.  
578 PubMed PMID: 12869497.

579 49. Trobridge GD, Wu RA, Beard BC, Chiu SY, Muñoz NM, von Laer D, Rossi JJ, Kiem HP. Protection of  
580 stem cell-derived lymphocytes in a primate AIDS gene therapy model after in vivo selection. *PLoS One*.  
581 2009;4(11):e7693. Epub 2009/11/06. doi: 10.1371/journal.pone.0007693. PubMed PMID: 19888329;  
582 PMCID: PMC2765621 which holds intellectual property on membrane-anchored anti-HIV C peptides.  
583 D.v.L. is co-inventor of membrane-anchored antiviral C peptides. J.J.R. is a Scientific Advisor to Benitec,  
584 Inc., an shRNA gene therapy company.

585 50. Hanawa H, Hematti P, Keyvanfar K, Metzger ME, Krouse A, Donahue RE, Kepes S, Gray J, Dunbar  
586 CE, Persons DA, Nienhuis AW. Efficient gene transfer into rhesus repopulating hematopoietic stem cells  
587 using a simian immunodeficiency virus-based lentiviral vector system. *Blood*. 2004;103(11):4062-9. Epub  
588 2004/02/21. doi: 10.1182/blood-2004-01-0045. PubMed PMID: 14976042.

589 51. Niwa H, Yamamura K, Miyazaki J. Efficient selection for high-expression transfectants with a  
590 novel eukaryotic vector. *Gene*. 1991;108(2):193-9. Epub 1991/12/15. doi: 10.1016/0378-1119(91)90434-  
591 d. PubMed PMID: 1660837.

592 52. Trobridge GD, Wu RA, Hansen M, Ironside C, Watts KL, Olsen P, Beard BC, Kiem HP. Cocal-  
593 pseudotyped lentiviral vectors resist inactivation by human serum and efficiently transduce primate  
594 hematopoietic repopulating cells. *Mol Ther*. 2010;18(4):725-33. Epub 2009/12/10. doi:  
595 10.1038/mt.2009.282. PubMed PMID: 19997089; PMCID: PMC2862537.

596

597

598

599

600

601

602

603

604

605

606

607

608

609

610

611

612



613 **FIGURE LEGENDS**

614

615 **Figure 1. TIM-4 binds to SIVGAGGFP infected CD4+ T cells.** A) Flow analysis of recombinant  
616 human TIM-4 binding to cells infected with SIVGAGGFP for 15 minutes (red), 1 hour (blue), or  
617 2 hours (orange). Lower plots show binding when gated on uninfected (SIVGAGGFP-) cells  
618 (left) or infected (SIVGAGGFP+) cells (right). B) Same experiment as in A without addition of  
619 TIM-4. Uninfected (SIVGAGGFP-) cells (left) or infected (SIVGAGGFP+) cells (right). C) TIM-4  
620 binding to CD4+ T cells incubated in the presence (blue) or absence (red) of 2  $\mu$ M camptothecin  
621 for 24 hours. D) Overlaid flow cytometry histograms of SIVGAGGFP infected CD4+ T cells in  
622 the presence (blue) or absence (red) of TAK779; uninfected CD4+ T cells are shown in orange  
623 (upper panel). Lower plots show binding when gated on uninfected (SIVGAGGFP-) cells (left) or  
624 infected (SIVGAGGFP+) cells (right).

625 **Figure 2. Assessment of CER T-cell potency in killing SIV infected cells.** A) Schematic  
626 diagram of the CER construct with the extracellular domain of TIM-4 linked to the TLR8  
627 signaling domain (CER21), CER21 with CXCR5 (CER21-CXCR5), the EGFR control vector  
628 (EGFR), and EGFR with CXCR5 (EGFR-CXCR5). B) Flow cytometry analysis of CD4+ and  
629 CD8+ T cells transduced with either CER21 or EGFR gated on expression of EGFR. Numbers  
630 in plots indicate the percentage of EGFR+ cells after gating on lymphocytes and singlets.  
631 Control untransduced CD4+ T cells are also shown. C) SIVGFP infected CD4+ T cells were  
632 mixed with CER T cells (green) or control EGFR T cells (green) at t=0. The E:T ratio was 5:1 for  
633 both CD4 (left) and CD8 (right) assays. Five images were taken in triplicate wells every 3 hours.  
634 The error bars indicate the standard error to the mean. D) Flow cytometry analysis of CD4+ T  
635 cells transduced with CER21-CXCR5 or EGFR-CXCR5 for expression of EGFR and CXCR5. E)  
636 Assessment of CER21-CXCR5 T-cell potency in killing SIV infected cells as described in C.

637 **Figure 3. Comparison of effector functions of diverse CERs.** A) Schematic diagram of 8  
638 CER constructs with the extracellular domain of TIM-4 linked to one or multiple intracellular  
639 signaling domains (ICD) originating from TLR8, TLR2, DAP10, DAP12, TRAF6, CD28 or CD3z;  
640 and negative controls without ICD (TIM-4–no ICD) or EGFR-CXCR5. B) CD4+ T cells  
641 transduced with CER lentiviruses. C) Assessment of CER T-cell potency in killing SIV infected  
642 cells as described. Five images were taken in triplicate wells every 3 hours. The error bars  
643 indicate the standard error to the mean. *P* values <0.05 for CER29, CER131, CER140, CER132  
644 and CER21 T cells compared with EGFR-CXCR5 T cells (Student's t-test). *P* values <0.05 for  
645 CER29, CER131, CER140 and CER132 T cells compared with TIM-4-no ICD T cells.

646 **Figure 4. CER131 containing TIM-4 PS binding site (PSBS) mutations lose ability to kill**  
647 **SIV infected CD4+ T cells.** A) Amino acid sequence of the wild-type TIM-4 FG loop including  
648 four residues important for PS binding (green). Residues replaced by alanine (brown) in CER-  
649 4A or deleted (blue) in CER– $\Delta$ BS. B) Flow cytometry analysis of CD4+ T cells transduced with  
650 CER131 WT and CER131 mutants for EGFR expression. C) Comparison of the potency of  
651 CD4+ T cells expressing CER131 WT (green), CER-4A (black) and CER– $\Delta$ BS (blue) in killing  
652 SIV infected cells as described in Figure 2C. The E:T ratio was 6:1.

653 **Figure 5. Additive killing activity of CER T cells and SIV directed CAR T cells against SIV**  
654 **infected CD4+ T cells.** A) Killing of SIV infected RM T cells by different ratios of CD4 CER and  
655 CD8 CAR T cells: EGFR CER with EGFR CAR T cells (red), CER21 with EGFR CAR T cells  
656 (green), CER21 with ITS06 CAR T cells (blue), and EGFR CER with ITS06 CAR T cells (gray)  
657 at E:T ratios indicated. Five images were taken in triplicate wells every 3 hours for all time  
658 points. B) Killing of SIV infected RM CD4+ T cells by the combination of CD4+ CER21 T cells  
659 and VRC26 CD3+ CAR T cells.

660

661

662 **Supplemental Material**

663 **Supplemental Figure 1. Generation of a fluorescent SIVmac239 virus.**

664



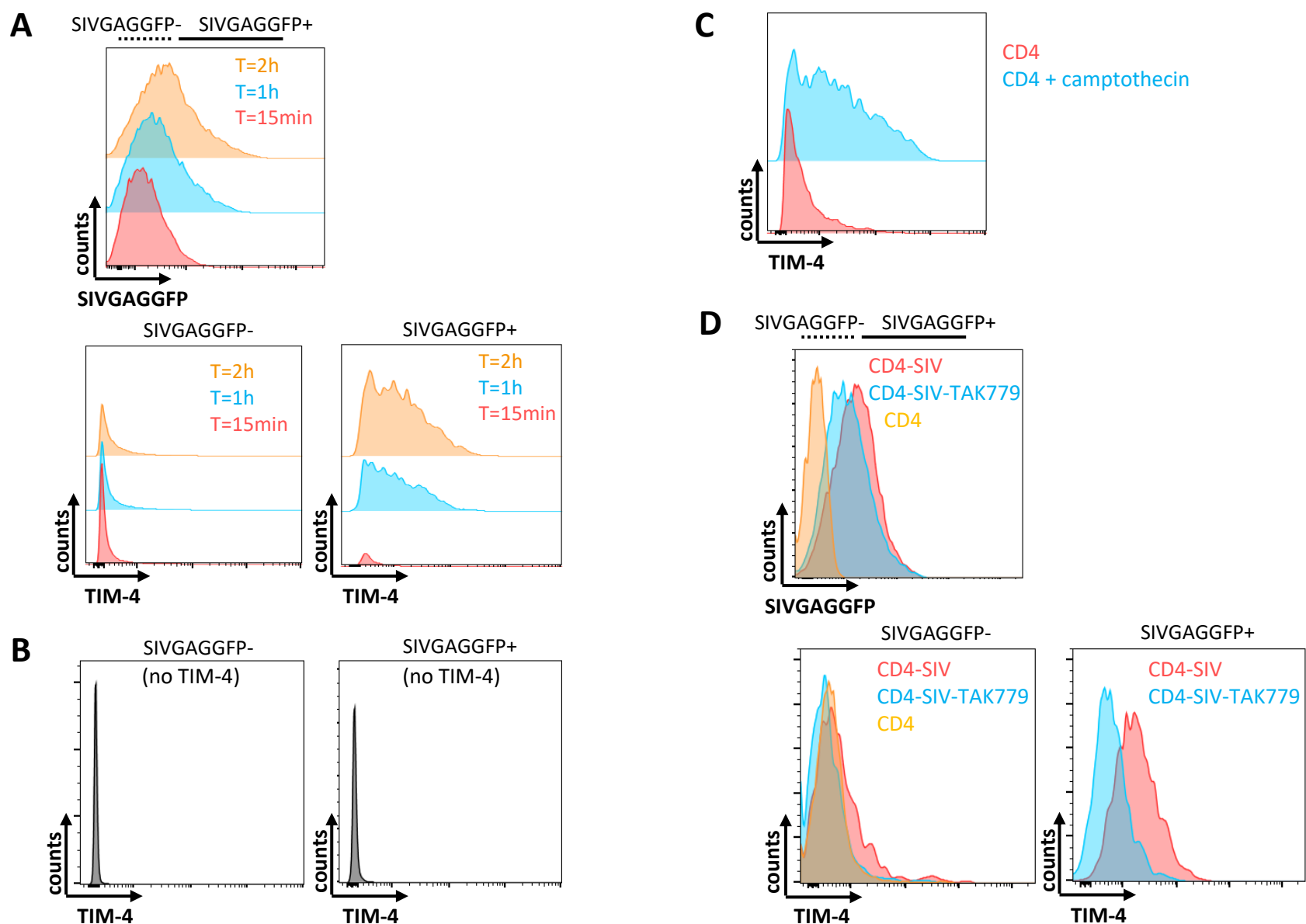


**Figure 1. TIM-4 binds to SIVGAGGFP infected CD4+ T cells.** A) Flow analysis of recombinant human TIM-4 binding to cells infected with SIVGAGGFP for 15 minutes (red), 1 hour (blue), or 2 hours (orange). Lower plots show binding when gated on uninfected (SIVGAGGFP-) cells (left) or infected (SIVGAGGFP+) cells (right). B) Same experiment as in A without addition of TIM-4. Uninfected (SIVGAGGFP-) cells (left) or infected (SIVGAGGFP+) cells (right). C) TIM-4 binding to CD4+ T cells incubated in the presence (blue) or absence (red) of 2 mM camptothecin for 24 hours. D) Overlaid flow cytometry histograms of SIVGAGGFP infected CD4+ T cells in the presence (blue) or absence (red) of TAK779; uninfected CD4+ T cells are shown in orange (upper panel). Lower plots show binding when gated on uninfected (SIVGAGGFP-) cells (left) or infected (SIVGAGGFP+) cells (right).

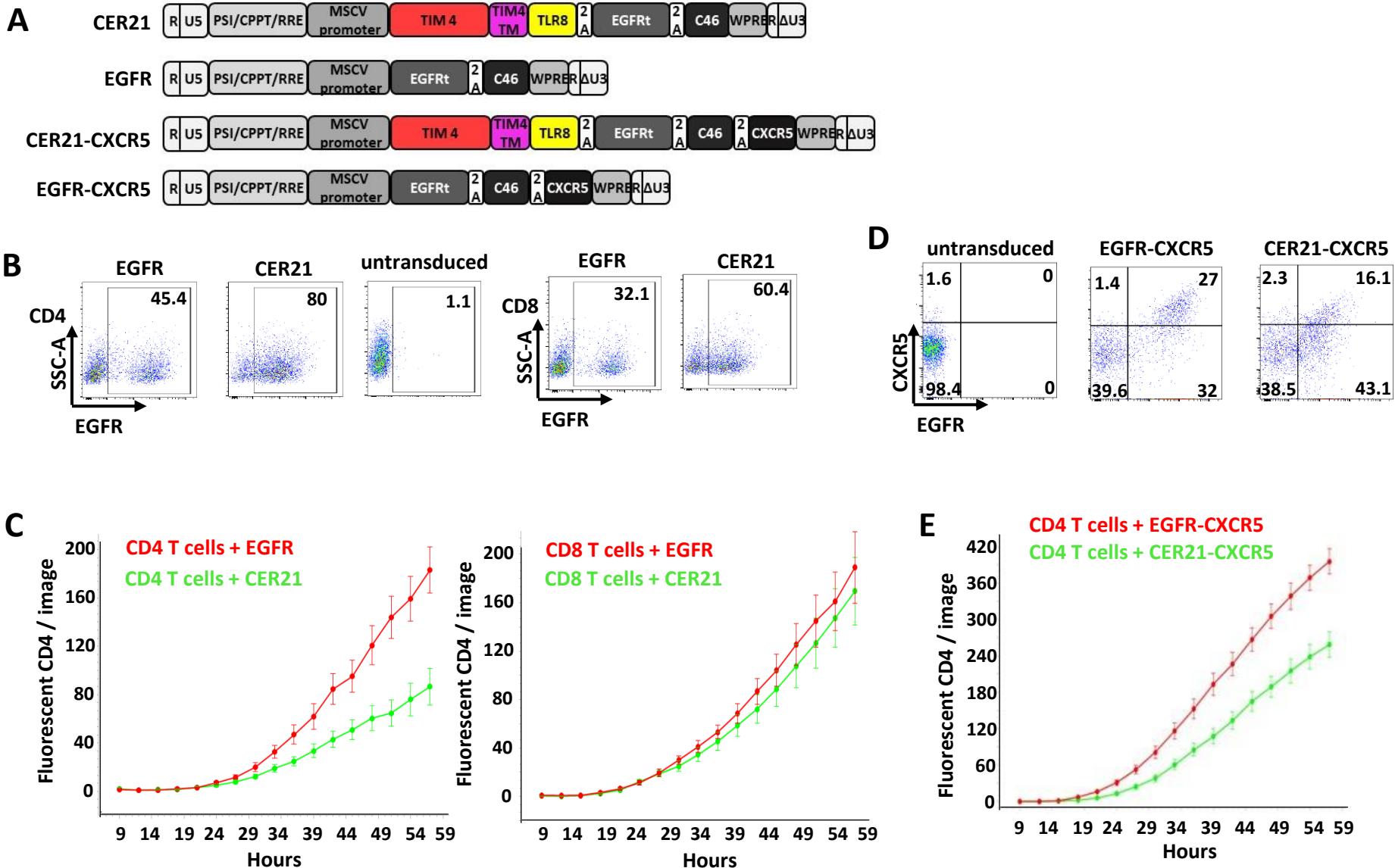
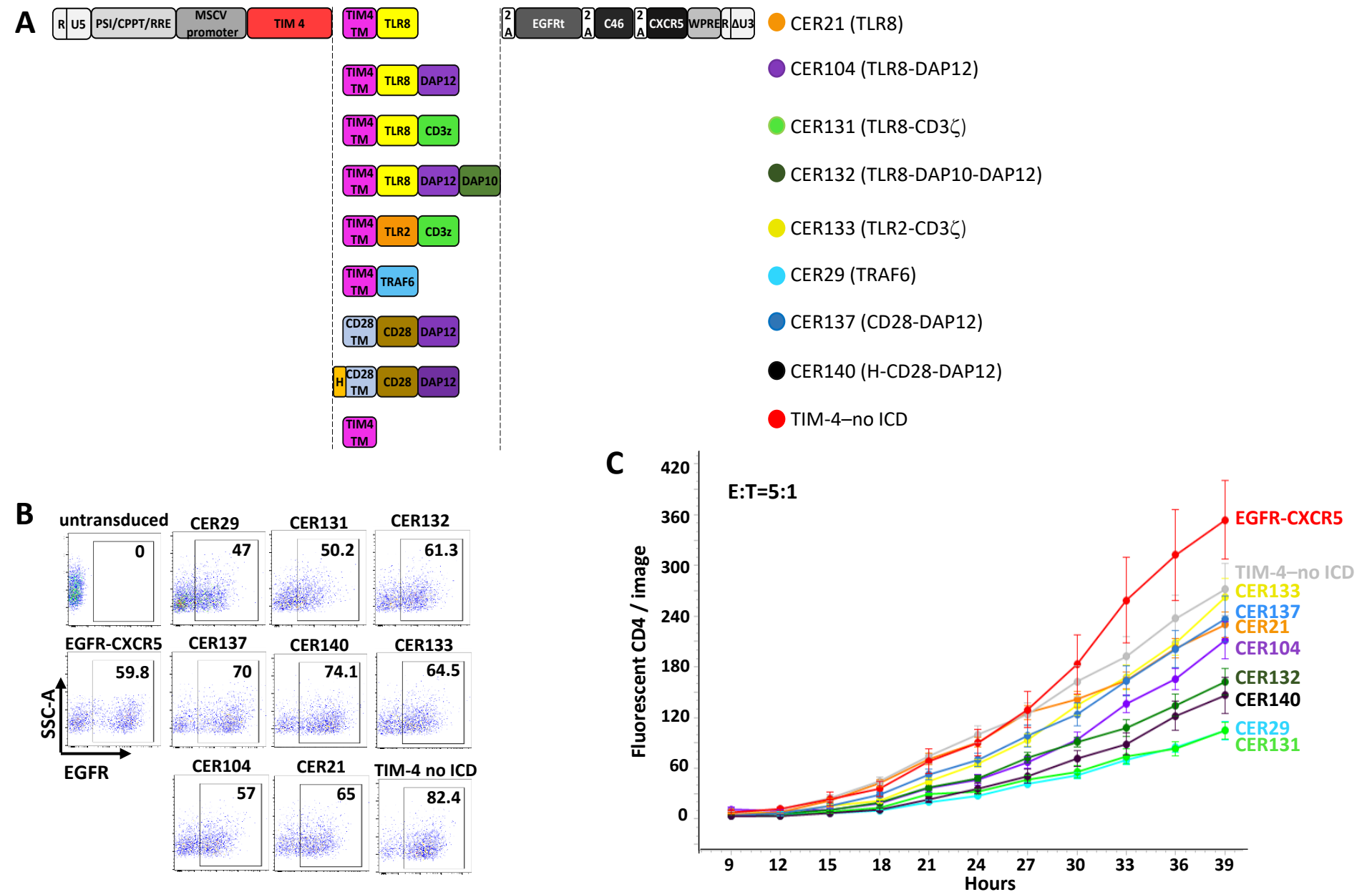


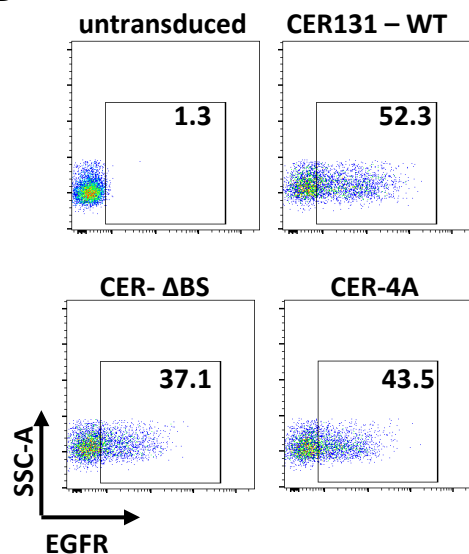
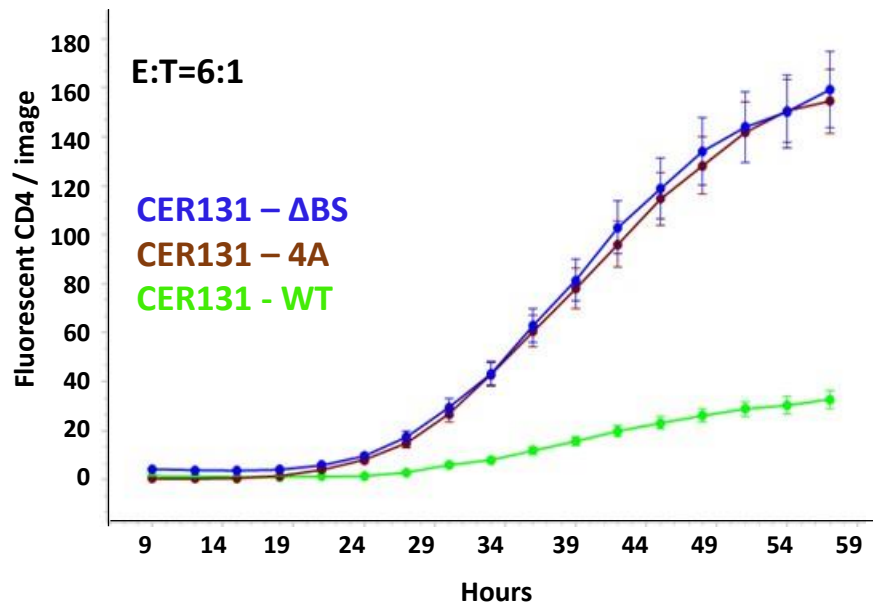
**Figure 2. Assessment of CER T-cell potency in killing SIV infected cells.** A) Schematic diagram of the CER construct with the extracellular domain of TIM-4 linked to the TLR8 signaling domain (CER21), CER21 with CXCR5 (CER21-CXCR5), the EGFR control vector (EGFR), and EGFR with CXCR5 (EGFR-CXCR5). B) Flow cytometry analysis of CD4<sup>+</sup> and CD8<sup>+</sup> T cells transduced with either CER21 or EGFR gated on expression of EGFR. Numbers in plots indicate the percentage of EGFR<sup>+</sup> cells after gating on lymphocytes and singlets. Control untransduced CD4<sup>+</sup> T cells are also shown. C) SIVGFP infected CD4<sup>+</sup> T cells were mixed with CER T cells (green) or control EGFR T cells (green) at t=0. The E:T ratio was 5:1 for both CD4 (left) and CD8 (right) assays. Five images were taken in triplicate wells every 3 hours. The error bars indicate the standard error to the mean. D) Flow cytometry analysis of CD4<sup>+</sup> T cells transduced with CER21-CXCR5 or EGFR-CXCR5 for expression of EGFR and CXCR5. E) Assessment of CER21-CXCR5 T-cell potency in killing SIV infected cells as described in C.



**A**

**PSBS: phosphatidylserine-binding site**

	F	G
<b>CER131 – wild type (WT)</b>	DSGVYCCRIEVPGWFNDVKINVRLNQRA	VKINVRLNQRA
<b>CER131 – mutated PSBS (CER-4A)</b>	DSGVYCCRIEVPGA <del>WFND</del> VKINVRLNQRA	VKINVRLNQRA
<b>CER131 - deleted PSBS (CER - ΔBS)</b>	DSGVYCCRIEVPG <del>WFNDVKINVRLNQRA</del>	VKINVRLNQRA

**B****C**

**Figure 4. CER131 containing TIM-4 PS binding site (PSBS) mutations lose ability to kill SIV infected CD4+ T cells.** A) Amino acid sequence of the wild-type TIM-4 FG loop including four residues important for PS binding (green). Residues replaced by alanine (brown) in CER-4A or deleted (blue) in CER-ΔBS. B) Flow cytometry analysis of CD4+ T cells transduced with CER131 WT and CER131 mutants for EGFR expression. C) Comparison of the potency of CD4+ T cells expressing CER131 WT (green), CER-4A (black) and CER-ΔBS (blue) in killing SIV infected cells as described in Figure 3C. The E:T ratio was 6:1.

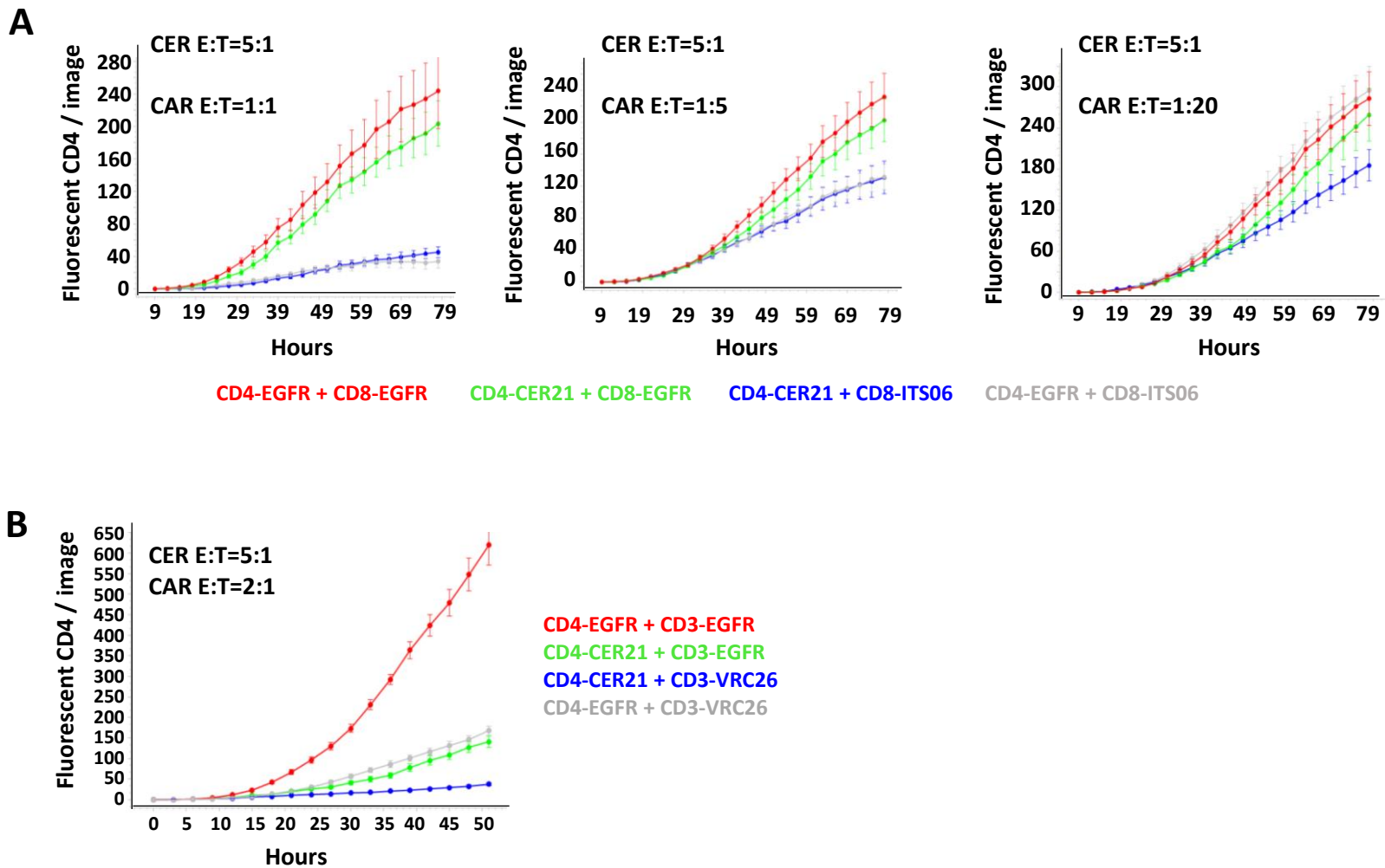


**Figure 5. Additive killing activity of CER T cells and SIV directed CAR T cells against SIV infected CD4+ T cells.** A) Killing of SIV infected RM T cells by different ratios of CD4 CER and CD8 CAR T cells: EGFR CER with EGFR CAR T cells (red), CER21 with EGFR CAR T cells (green), CER21 with ITS06 CAR T cells (blue), and EGFR CER with ITS06 CAR T cells (gray) at E:T ratios indicated. Five images were taken in triplicate wells every 3 hours for all time points. B) Killing of SIV infected RM CD4+ T cells by the combination of CD4+ CER21 T cells and VRC26 CD3+ CAR T cells.